Monika LEWANDOWSKA[1], Kamil SEDLAK[2]

West Pomeranian University of Technology, Szczecin (1), EPFL-CRPP, Villigen PSI (2)

Thermal-hydraulic analysis of the improved LTS conductor design concepts for the DEMO TF coil

Abstract. The improved design concepts for the LTS TF coil system of DEMO have been proposed in 2013 by EPFL-CRPP PSI Villigen and ENEA Frascati. The present study is focused on the thermal-hydraulic analysis of the conductor designs, which includes: hydraulic analysis, heat removal analysis and assessment of the maximum temperature and the maximum pressure in each conductor during quench.

Streszczenie. W 2013 r. zespoły z EPFL-CRPP i ENEA Frascati opracowały udoskonalone koncepcje projektowe kabli dla poszczególnych warstw cewki TF tokamaka DEMO. W pracy przedstawiono analizę cieplno – przepływową projektów kabli obejmującą: analizę hydrauliczną, oszacowanie zdolności usuwania ciepła oraz oszacowanie maksymalnej temperatury oraz maksymalnego ciśnienia podczas utraty stanu nadprzewodzenia.. (Analiza cieplno-przepływowa udoskonalonego projektu kabli nadprzewodnikowych dla cewki TF tokamaka DEMO).

Keywords: thermal-hydraulic analysis, low T_c superconductors, quench, TF coil, DEMO
Słowa kluczowe: analiza cieplno-przepływowa, nadprzewodniki niskotemperaturowe, utrata stanu nadprzewodzenia, cewka TF, DEMO.

Introduction

Long–term efforts of the European community towards the realization of fusion energy are currently focused on the design of DEMO - a demonstration fusion power plant producing net electricity for the grid at the level of a few hundred MW. It is foreseen that DEMO will start operation in the early 2040s [1]. The core of DEMO is an inductively driven tokamak with 16 toroidal field (TF) coils and the major radius of about 9 m [2]. Current design and assessment studies in the superconducting magnets for DEMO include activities both on low (LTS) and high (HTS) T_c superconductors, as well as engineering integration. LTS technology is fully mature, so the related activities are focused on the design and construction of coils which would fulfil the specific DEMO requirements. A parallel HTS R&D program includes studies, testing and development of different HTS cable concepts, such as e.g. twisted stack cable, Roebel assembled coated conductor (RACC) or conductor on round core (CORC), for possible future application to fusion [3]. Our work is a part of LTS activities.

Two preliminary design concepts for the LTS TF coil system of DEMO have been proposed in 2012 by EPFL-CRPP PSI Villigen and ENEA Frascati [4]. The mechanical, electromagnetic and thermal-hydraulic analyses of the both preliminary design concepts revealed that they required some modifications. The improved design concepts have recently been proposed [2] and subjected to comprehensive analyses. The present work is focused on the thermal-hydraulic analysis of both candidate designs. The feedback from the analysis results will lead to further optimization of the conductor layouts in the next iteration of the design.
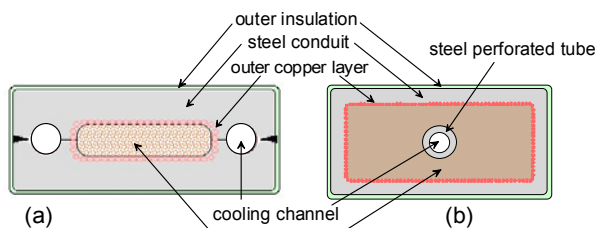

Fig.1. Schematic layout of (a) CRPP and (b) ENEA conductor.

Conductors' characteristics and model assumptions

The LTS TF coil designed for DEMO consists of nine graded double layers (DLs) wound using:
 a) CRPP design: "react & wind", flat multistage cables with two side cooling channels (Fig. 1a),

 b) ENEA design: "wind & react", rectangular CICC with a central cooling channel separated from the bundle region with a thick steel perforated tube (Fig. 1b).
The six inner DLs (DL1-DL6) located in a high magnetic field region, are made of Nb_3Sn superconductors, whereas the three outer DLs (DL7-DL9) are made of NbTi. The conductors' parameters relevant for the present analysis, are presented in Table 1. In the 2nd column we show the lengths, L, of the inner (shortest) conductor in each DL. We calculated the effective bundle void fraction, φ, listed in the 3rd column, under the assumption that the outer copper layer is a part of of the bundle.

Table 1. Conductors' characteristics used in the analysis

DL	L (m)	φ (-)	$D_{h,B}$ (mm)	$A_{He,B}$ (mm²)	A_{sc} (mm²)	A_{Cu1} (mm²)	A_{Cu2} (mm²)	A_{steel} (mm²)	B_0 (T)	T_{cs} (K)
CRPP design										
1	438	0.19	0.91	227	276	276	413	3272	13.24	6.99
2	445	0.19	0.92	203	162	162	536	3290	11.86	6.42
3	452	0.19	0.92	195	126	126	559	3237	10.89	6.26
4	459	0.19	0.92	195	114	114	584	3127	10.07	6.51
5	543	0.19	0.92	183	94	94	575	2650	9.24	6.40
6	551	0.19	0.92	183	82	82	599	2650	8.12	6.80
7	559	0.28	0.92	437	265	397	487	2016	6.91	5.61
8	566	0.27	0.93	375	160	400	436	2161	5.68	6.01
9	492	0.27	0.93	375	160	400	436	2044	4.15	6.77
ENEA design										
1	512	0.25	0.54	486	353	353	696	1858	13.08	6.31
2	520	0.24	0.53	470	203	203	991	1853	11.43	6.16
3	528	0.24	0.53	419	151	151	941	1764	10.21	6.23
4	536	0.24	0.53	396	127	127	944	1748	9.33	6.40
5	544	0.24	0.53	396	101	101	980	1740	8.27	6.48
6	552	0.24	0.53	388	75	75	1017	1735	7.11	6.30
7	440	0.27	0.60	531	411	616	336	2044	5.80	6.32
8	446	0.27	0.59	492	91	137	1046	2021	4.80	6.12
9	410	0.27	0.59	437	46	68	1030	1907	3.57	6.09

Symbol $D_{h,B}$ denotes the hydraulic diameter of the bundle, A is the cross section of different cable components: helium in the bundle (index He,B), superconductor (index sc), steel and copper, B_0 is the expected maximum magnetic flux density at the nominal operating current I_0 [5], and T_{cs} is the value of the current sharing temperature expected at B_0 [5]. In both designs copper in superconducting strands (index Cu1) has RRR of 100, whereas copper in segregated strands and in the outer layer (index Cu2) is characterized by RRR = 400 and 300 in

the CRPP and ENEA design, respectively. The inner diameter of the cooling channel is D_{in} = 6 mm for all ENEA conductors, whereas in the CRPP design D_{in} = 10 mm for the conductors in DL1 and 6 mm in the rest of DLs. The diameter of cooling channels is increased in the CRPP DL1 conductors, since they will be subjected to the highest heat deposition due to nuclear radiation during the plasma burn.

We assume that the coil is cooled by the forced flow of supercritical helium at nominal inlet conditions p_{in} = 0.6 MPa, T_{in} = 4.5 K, and that the expected value of the pressure drop in the coil at operating conditions is Δp = 0.1 MPa. These cooling conditions are similar to those of ITER.

Our thermal-hydraulic analysis of both candidate conductor designs includes:
a) hydraulic analysis – calculation of the mass flow rates in each conductor at the expected value of pressure drop in the coil and assuming no heat deposition in the coil (such conditions occur during the dwell time),
b) heat removal analysis – calculation of mass flow rates and the helium temperature profile in each conductor as functions of heat deposition rate,
c) calculation of the temperature and pressure evolution in each conductor during quench, using two different tools, namely: (i) a simplified 0-D model representing the extreme scenario for the maximum pressure: whole conductor is in normal state and all channels of flow are blocked, and (ii) a more realistic 1-D model of quench development, obtained using the code THEA [6].

The simplified models adopted in the hydraulic, heat removal and quench analysis are similar to those used in our study of the preliminary conductors' designs proposed in 2012. These models were described in detail, including the governing equations, in [7].
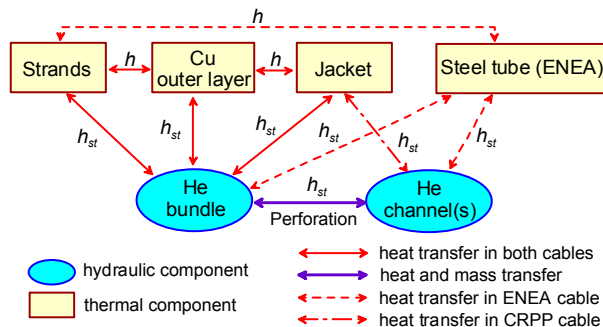

Fig. 2. Thermal and hydraulic components defined in the THEA model and their interactions

The THEA model of each conductor consists of several parallel 1-D components (see Fig. 2). The heat transfer coefficient h between the adjacent thermal (solid) components is set to 100 W/m^{2}K. The heat transfer coefficients, h_{st}, between hydraulic and thermal components are computed using the standard heat transfer correlations for the flow in smooth tubes, namely: Nusselt number Nu = 4 for the laminar flow and the Dittus-Boelter correlation for the turbulent flow. This approach should provide conservative (underestimated) values of h and h_{st}. To assess friction factors for the flow in cooling channels we apply the standard smooth tube correlations, whereas for the flow in bundle regions we use the correlations based on the porous medium analogy proposed in [8] and [9]. For the final calculations we decided to use only the correlation taken from [8], which appeared to be more conservative.

In the THEA quench simulations we studied two cases of the magnetic field distribution along the cable (see Fig. 3), leading to two different quench initiation scenarios. In

Case A the magnetic field along the cable is kept constant and equal to 12.74 T (slightly below B_0), except the 10 m long region around x = 300 m where the field follows the profile resulting from the magnetic field analysis performed in 2012 [10]. The peak-like magnetic field profile (Case A) should lead to local quench initiation, and consequently to the highest hot-spot temperature. The constant magnetic field distribution (Case B) should cause almost simultaneous quench initiation along the full cable length, which corresponds to the higher maximum pressure than in Case A, however, the maximum temperature should be lower than in Case A, due to the faster quench detection.
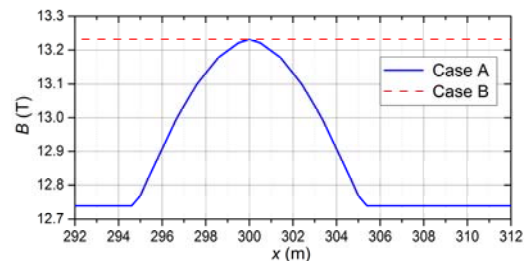

Fig. 3. Magnetic field profile along the conductor at operating current I_0 assumed in the quench analysis.

The initial temperature of all the cable components is set slightly (about 0.1 K) above T_{cs}. For each conductor, at first the current is set equal to zero and the simulation is carried out until the steady state is reached. Then the stationary temperature, pressure and mass flow rate profiles along the cable are saved and later serve as the initial state for the subsequent quench simulations. At the beginning of a quench simulation the current is switched on to the operating value I_0 = 82.4 kA. Because the temperature of superconductor is above T_{cs} (within a short region of conductor (Case A) or along the full conductor length (Case B)), the resistive voltage over the full conductor length starts to increase and at time $t_{detection}$ it reaches the threshold value of 0.5 V. Then the fast discharge procedure is triggered. The operating current and the magnetic field are dumped according to the equations:

$$(1) \qquad I(t) = \begin{cases} I_0 & \text{for } t \le t_{delay} \\ I_0 \cdot \exp\left[-(t - t_{delay})/\tau\right] & \text{for } t > t_{delay} \end{cases},$$

$$(2) \qquad B(t) = B_{initial}\, I(t)/I_0,$$

where τ = 23 s is the decay time constant for current dump [4], and t_{delay} is the time at which the current dump starts, conservatively assumed to be $t_{delay} = t_{detection}$ + 2 s [11]. We have checked that small variations of the initial temperature may lead to large variations of $t_{detection}$, however, the resulting maximum quench temperature is not affected significantly by the choice of the initial temperature.
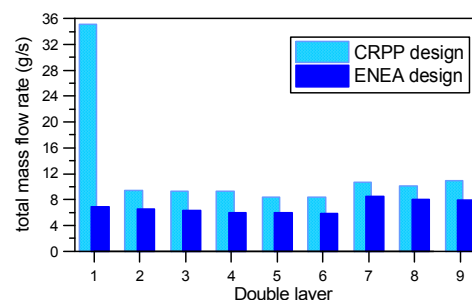

Fig. 4. Total mass flow rates in the shorter conductor in each DL of CRPP and ENEA coil (no heat deposition in the coil).

Results

The results of the hydraulic analysis are presented in Fig. 4. It is seen that the total helium mass flow rate in ENEA conductors is smaller than in the respective CRPP conductors, particularly in DL1, despite the fact that the ENEA design is characterized by larger total helium cross sections as compared to the CRPP design. This is because most of helium flows in cooling channels, which are diameter of cooling channels in the CRPP DL1 conductors is particularly large. The total mass flow rate in the TF coil, in case when there is no heat deposition, was assessed to characterized by low hydraulic impedance. The helium cross section in cooling channels is larger in CRPP conductors, which have two cooling channels and the diameter of the cooling channels in the CRPP DL1 conductors is particularly large. The total mass flow rate in the TF coil, in case when there is no heat deposition, is assessed to be 224 g/s and 124 g/s for the CRPP and ENEA design, respectively.

The results of the heat removal analysis are presented in Figs. 5a – 5b and in Table 2. It is seen that the outlet helium temperatures increase with the heat deposition rate, $\dot{Q}$, as expected. The outlet helium temperatures in the ENEA conductors are higher than in the respective CRPP conductors, which indicates that the heat removal capability of the ENEA coil is poorer as compared to the CRPP coil. The expected nuclear heat deposition in the DL1 is of about 100 W [4]. The safe operation of a cable is ensured if the temperature margin is sufficiently large (T_{cs} - T_{out} > 1.5 K). In Table 2 we show the values of the helium outlet temperature in the inner conductor of DL1 calculated for the heat deposition rate 100 W (the most pessimistic scenario – all power deposited in the inner conductor) and 50 W (heat deposited evenly in both conductors of DL1). It is seen that the temperature margin in the ENEA DL1 conductor is too small, even at the smallest assumed heat deposition.

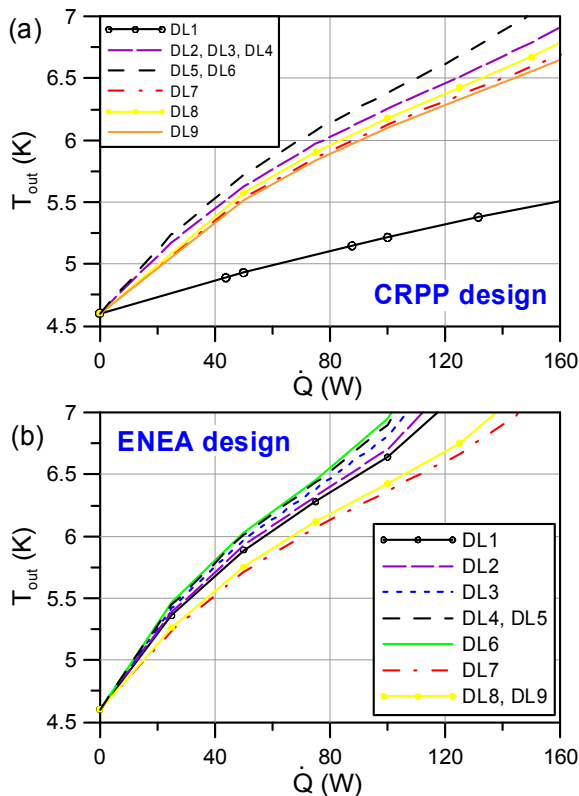(a) CRPP design

(b) ENEA design

Fig. 5. The outlet helium temperature for the shorter conductor in each DL as a function of heat deposition rate

Table 2. The outlet helium temperature for the inner conductor in the first DL for the expected heat deposition rate

Design	T_{cs} (K)	$\dot{Q}$ = 50 W		$\dot{Q}$ = 100 W	
		T_{out} (K)	T_{cs} -T_{out} (K)	T_{out} (K)	T_{cs} -T_{out} (K)
CRPP	6.99	4.93	2.06	5.22	1.77
ENEA	6.31	**5.89**	**0.42**	6.64	-0.67

Typical results of THEA quench simulations are presented in Figs. 6a-6b, whereas the maximum quench temperatures and pressures resulting from different models are compiled in Table 3. It is seen that for all ENEA conductors and CRPP NbTi conductors (DL7-DL9) theresults of THEA simulations do not depend significantly on the scenario of quench initiation. For these conductors also the values of the maximum quench temperature obtained with the simplified model, which assumes instantaneous heat transfer between different cable components, are close to those resulting from the THEA simulations, despite the conservative values of heat transfer coefficients used in the
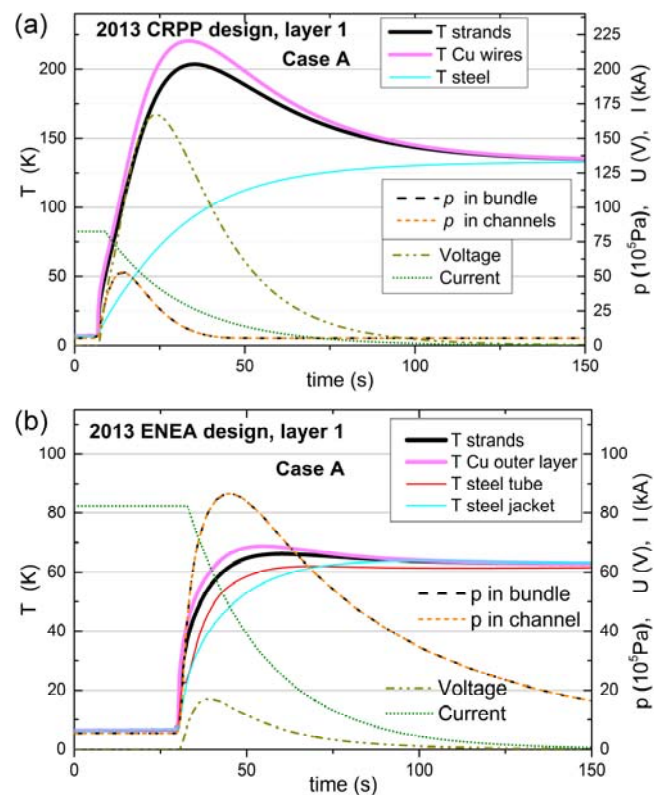

Fig. 6. Quench evolution in the DL1 cables simulated with THEA. Temperature and pressure are computed in the middle of the normal zone.

Table 3. Maximum temperature and pressure in the DEMO TF conductors calculated with the simplified model and with THEA.

DL	Simple model		THEA Case A		THEA Case B	
	T_{max} (K)	p_{max} (MPa)	T_{max} (K)	p_{max} (MPa)	T_{max} (K)	p_{max} (MPa)
CRPP design						
1	68	16.6	214	5.8	220	5.3
2	65	16.1	220	11.5	244	9.3
3	65	16.0	237	11.8	273	9.2
4	63	15.6	227	10.4	266	7.6
5	70	17.2	266	12.3	322	9.3
6	66	16.3	250	10.1	309	6.6
7	53	13.0	62	9.6	67	9.4
8	54	13.1	73	9.4	85	8.9
9	46	11.0	63	7.3	76	6.7

ENEA design					
1	58	14.1	64	9.7	69	8.7
2	51	12.3	51	8.9	61	7.4
3	54	13.1	58	8.7	69	7.4
4	53	13.0	58	7.9	70	6.8
5	51	12.4	55	7.3	68	6.1
6	48	11.7	52	6.9	66	5.7
7	47	11.4	46	7.0	46	6.1
8	38	9.0	37	6.0	38	5.1
9	38	8.9	37	5.8	37	4.8

THEA model. For the CRPP DL1-DL6 conductors with relatively small copper cross section (which implies huge Joule heat generation in copper during quench), and particularly large steel cross section, the assumption of perfect heat transfer between different cable components is not justified. In these conductors significant temperature differences between different cable components are observed in THEA simulations (see Fig. 6a). As a result, for CRPP DL1-DL6 conductors there is a large discrepancy between the maximum quench temperatures resulting from different approaches. In particular, the maximum quench temperatures obtained with the simplified model are much lower than those resulting from THEA simulations.

The maximum strand temperature in CRPP DL1-DL6 conductors during quench are relatively high (above 200 K). The ITER Design Description Document [12] indicates that the strands inside the jacket "*may reach up to 250 K on a transient basis, as it is mechanically flexible and can absorb the differential expansion with the jacket by compressive strain*". The maximum strand temperatures in the CRPP DL2-DL6 conductors are close to or even above this 250 K criterion. We suggest to include additional copper wires in the cable bundles of DL2-DL6 in the next conductor design iteration. This change should lead to reduction of both maximum quench temperature and pressure.

Conclusions

The performed thermal-hydraulic analysis of the improved designs of the LTS DEMO TF coil revealed that both CRPP and ENEA designs require some modifications in the next iteration of the design. To increase the heat removal capability and the related temperature margin we suggest to increase the diameter of the central cooling channel in the ENEA DL1 conductor. The copper cross section in the CRPP DL2-DL6 conductors should be increased to reduce the maximum quench temperature. On the other hand, the amount of copper could be potentially decreased in ENEA conductors. Pressures developed during the quench, which are around 10 MPa, are relatively high, however still manageable within today's technology. They could be lowered by enlarging the opening of cooling channels, however, at the expense of increased amount of supercritical helium, which could be demanding for the DEMO cryogenic system.

Authors: *dr hab. inż. Monika Lewandowska, Institute of Physics, Faculty of Mechanical Engineeering and Mechatronics, West Pomeranian University of Technology, Szczecin Al. Piastów 48, 70-311 Szczecin, Poland, E-mail: monika.lewandowska@zut.edu.pl, Dr. Kamil Sedlak, EPFL-CRPP, Fusion Technology Division, CH-5232 Villigen-PSI, Switzerland, E-mail: Kamil.Sedlak@psi.ch*

REFERENCES

[1] Romanelli F., Barabaschi P., Borba P., *et al.*, A roadmap to the realization of fusion energy, EFDA, Garching, Germany, 2012.
[2] Bruzzone P., Sedlak K., Stepanov B., Muzzi L., Turtù S., Anemona A., Harman J., Design of large size, force flow superconductors for DEMO TF coils, *IEEE Trans. Appl. Supercon.*, 24 (2014), No. 5, 4201504 (4 pp.)
[3] Fietz W.H., Barth Ch., Drotziger S., Goldacker W., Heller R., Schlachter S.I., Weiss K.-P., Prospects of High Temperature Superconductors for fusion magnets and power applications, *Fus. Eng. Des.*, 88 (2013) 440– 445
[4] Bruzzone P, Sedlak K, Stepanov B., High current super-conductors for DEMO, Fus. Eng. Des. 88 (2013), 1564 -1568
[5] Sedlak K., Electromagnetic and quench bahaviour of candidate prototype LTS conductor, Report to EFDA task WP-13-DAS01-T03a, 2013 (unpublished)
[6] Bottura L., Rosso C., Breschi M., A general model for thermal, hydraulic and electric analysis of superconducting cables, *Cryogenics*, 40 (2000) 617–626
[7] Lewandowska M., Sedlak K., Thermal-hydraulic analysis of LTS cables for the DEMO TF coil, *IEEE Trans. Appl. Supercon.*, 24 (2014), No. 3, 4200305 (5 pp.)
[8] Bagnasco M., Bottura L., Lewandowska M., Friction factor correlation for CICC's based on a porous media analogy, *Cryogenics* 50 (2010) 711-719
[9] Lewandowska M., Bagnasco M., Modified friction factor correlation for CICC's based on a porous media analogy, *Cryogenics* 51 (2011) 541-545
[10] Muzzi L., Turtù S., ENEA draft report on magnetic field calculation, Report to EFDA task WP12-DAS01-T04, 2012 (unpublished)
[11] Marinucci C., Calvi M., Bottura L., Bruzzone P., Herzog R., Quench analysis of the European High Field Superconducting Dipole Magnet EDIPO, *IEEE Trans. Appl. Supercon.*.18 (2008) 200-203
[12] ITER design description document. Magnets. Section 1: Engineering description, ITER_D_22HV5L v2.2, 2006.